Journal of Cranio-Maxillo-Facial Surgery 42 (2014) 283–289

Contents lists available at SciVerse ScienceDirect

Journal of Cranio-Maxillo-Facial Surgery

journal homepage: www.jcmfs.com

Computer-aided orbital wall defects treatment by individual design ultrahigh molecular weight polyethylene implants☆

Marcin Kozakiewicz*

Department of Maxillofacial Surgery (Head: Marcin Kozakiewicz, DDS, PhD), Medical University of Lodz, Zeromskiego 113, Lodz, Poland

ARTICLE INFO

Article history:
Paper received 1 November 2012
Accepted 23 May 2013

Keywords:
Orbit
CAD
CAM
Ultrahigh molecular weight polyethylene

ABSTRACT

Despite of well-known advantages of high molecular weight polyethylene (Medpor, Synpore) in orbital reconstructions, the thickness of those implants significantly exceeds 0.5 mm and precise modification of thickness is limited. The aim of this study was to present the application of a selfdeveloped method of treatment orbital wall fracture by custom implant made of ultrahigh molecular weight polyethylene (UHMW-PE).

Material and method: First, the test of influence of sterilization process upon implant deformation was performed (autoclaving, ethylene oxide, gas plasma, irradiation). Next, ten cases for delayed surgical treatment of orbital fracture were included into this study (7 males, 3 females). Based on CT scan and mirrored technique, a CAD model of virtual implant for repairing orbital wall was made. Then, an implant was manufactured with a computer numerical controlled milling machine from UHMW-PE block, sterilized and used during a surgical procedure. Clinically used implants had thickness from 0.2 to 4.0 mm.

Results: The best method of sterilization is ethylene oxide process, and the worst is autoclaving. In this series of delayed surgical cases, functional results of orbital surgery are worse than in simpler, early treated cases, but long-term subsidence of diplopia is noticeable [10% poor results]. The results of the treatment depend on the initial level of diplopia where severe initial diplopia to be corrected requires thicker implants ($p < 0.01$). It also leads to longer surgical procedures ($p < 0.01$), but prolongation of the surgery had no negative influence upon results of any investigated follow-up examinations. Obviously, the orbital destruction intensity is related to injury-evoked initial diplopia but it also influences whole results of treatment up to 12 months post-op. Interesting result is presented by the relation of maximal implant thickness to 12-month diplopia evaluation. Thicker implants used result in lower residual diplopia ($p < 0.05$). This is important because of the correlation between the higher orbital destruction intensity with a thicker UHMW-PE implant ($p < 0.05$) applied in this series.

Conclusion: Patient-specific ultrahigh molecular weight polyethylene implants enable precise reconstructions of orbital wall. One should not be afraid of a significant eye globe reposition caused by these thickness modulated implants, as such repositioning is essential for an efficient correction of enophthalmos.

1. Introduction

Orbital wall fractures and defects are still among the leading topics in maxillofacial surgery (Betz et al., 2010; Wu et al., 2011). The most common causes of orbital fracture are falls, assaults, traffic accidents and sporting events. Periorbital ecchymosis (88%), diplopia (66%), hypoesthesia in the n.V_2 distribution (54%) and intra-orbital emphysema (42%) are the most common signs and symptoms (Brady et al., 2001). Later enophthalmos becomes the most disfiguring symptom (Hoşal and Beatty, 2002; He et al., 2012). Open reduction and reconstruction is the method of treatment in case of isolated inferior orbital wall fracture (i.e. blowout fracture). From 2006 individual implants have been used in this area of maxillofacial surgery (Schön et al., 2006; Kozakiewicz et al., 2009). The method is very promising because of predictable ophthalmological results (Kozakiewicz et al., 2011, Loba et al., 2011; He et al., 2012).

High-density polyethylene (HDPE) implants in the facial skeleton are used to restore anatomical harmony following accidental or iatrogenic trauma, to correct congenital deformities or in

☆ Study was presented in Custom Models Session during XXI Congress of EACMFS at Dubrovnik, Croatia, September 11–16th, 2012.

* Tel.: +48 42 6393738; fax: +48426393739.
E-mail addresses: marcin.kozakiewicz@umed.lodz.pl, mm_kk@toya.net.pl.

1010-5182/$ – see front matter © 2013 European Association for Cranio-Maxillo-Facial Surgery. Published by Elsevier Ltd. All rights reserved.
http://dx.doi.org/10.1016/j.jcms.2013.05.015

aesthetic surgery (Frodel and Lee, 1998, Liu et al., 2004). HDPE has shown to be an excellent alloplastic bony replacement material and seems to be very effective for skeletal replacement in non-load-bearing regions. It is used as the material of choice for orbital reconstruction in both the primary and secondary setting, with a growing confidence in the use of the material even in patients requiring radiotherapy (Hwang et al., 2009; Xu et al., 2009; Rhim et al., 2010; Kashkouli et al., 2011; Kirby et al., 2011). Results are comparable to autogenous bone reconstruction (Wajih et al., 2011). The rate of complication attributable to the material is only 6.4% (Lee et al., 2005). The thickness of the implant sheet usually exceeds 0.5 mm which makes it impossible to meet requirements of thin implant reconstruction and precise modification of its thickness. On the other hand, sandwich onlays with manual suturing are performed in double or multilayer reconstruction (Tabrizi et al., 2010). In the proposed ultrahigh molecular weight polyethylene (UHMW-PE) implants the problem of variable thickness is resolved (Kozakiewicz et al., 2013).

The aim of this study is to present the application of a method of orbital wall fracture treatment by custom implant made of UHMW-PE developed in our department.

2. Material and methods

A test implant was designed and manufactured to validate the process of sterilization (Fig. 1B). Its design dimensions were: 23 mm width, 34 mm long, depth of concavity 5.5 mm and thickness 0.5 mm. The upper base was flat. The design goal for the shape was to facilitate measurement of the dimensions and to find deformations. The weight according the CAD was 0.27 g, volume 288.23 mm^3 and total surface was 1,201.26 mm^2. 40 test implants were manufactured by a computer numerically controlled (CNC) milling process from medical certified UHMW-PE (Fig. 1A, C), marked and measured. Each test implant was measured three times and then an average was calculated and recorded in a spreadsheet. Samples were cleaned ultrasonically, dried, packed in paper-foil envelopes and sealed. Four sterilization processes were used, typical for hospital work. 1. Autoclaving at a temperature of 134 °C and 2 atm pressure in 1 h cycle. 2. Ethylene oxide at. 55 °C, $t = 4.5$ h + degasation time 12 h. 3. Hydrogen peroxide gas plasma at. 55 °C and 0.02 atm pressure in 1 h cycle. 4. Radiation in an electron beam 7 MeV, 35 °C, total dose per test implant 25 kGy in 1 h cycle. The implants were divided into four ten-item groups, one for each sterilization method. Measures of test implants were once again made after sterilization and statistical evaluation of pre- vs. post-sterilization dimensions was performed by *t*-test (normal distribution) or sign test (other than normal distribution) for paired samples. The level of significance was established as $p < 0.05$.

In this study 10 consecutive subjects were included (7 males, 3 females) who had sustained orbital fractures and were referred mainly for delayed surgical reduction (Table 2). Ethical Committee permission was obtained (RNN/266/11/KB). Previous surgical treatment had been performed in 7 of the10 cases. Our surgical procedure was performed 1.96 ± 0.92 year later. The average patient age was 28 ± 3.6 year.

Multi-slice VCT, using a GE Lightspeed 64-slice scanner (GE Healthcare, United Kingdom), (0.6 mm layers, gantry tilt 0° matrix) was performed for all patients on the day of admission to hospital. Diagnosis was established in all cases on the basis of maxillofacial and ophthalmological examination and computerized tomography. Inclusion criteria were diplopia or significant enophthalmos (>4 mm) or a large fracture on a computed tomographic scan (>50% of at least one orbital wall area).

Injury effects were classified by an orbital destruction intensity (ODI) scale (Kozakiewicz et al., 2011). The scale is described as follows: 1. site of destruction: floor i.e. one wall (1W); 2. floor + one wall medial or lateral (i.e. two walls 2W); 3. floor + one margin i.e. one wall and one orbital margin (1W+1M); 4. floor + one wall + one margin i.e. 2W + 1M; 5. floor + one wall + two margins i.e. 2W + 2M; 6. floor + two walls + one margin i.e. 3W + 1M; 7. floor + one or two walls + two margins i.e. 3W + 2M; 8. floor + two or three walls + more than two margin i.e. 3–4W + 3–4M. All patients underwent full ophthalmic and orthoptic assessment 1 month post-operatively. None of the patients had a history of binocular vision impairment prior to the injury. The extent of diplopia was assessed on the binocular single vision BSV screen (Medmont M700) with the examination field extending 30° superiorly and 40° inferiorly. The results of this method (BSV loss) were presented as a percentage of the examined visual field in which the patient reports double images. For statistical reasons the range 0–100% was converted into 0–1.

Assessment of CT examinations was carried out and the volume of interest i.e. both orbits and the surrounding bone structures were determined. Relevant DICOM data from these studies were the basis for creating virtual models in Geomagic Studio 12 (Geomagic Corp., Morrisville, USA). The unaffected orbit was mirrored onto the contralateral side i.e. the injured orbit. Radiological and maxillofacial consultation was necessary at this point. It was important to determine the orbital wall destruction area for proper implant design. Next, the left-right reference (symmetrical) surfaces on the orbital rim were identified to find the best site for implant fixation – Geomagic Qualify (Geomagic Corp., Morrisville, USA). Following this, the anterior part of the virtual implant was superimposed onto the reference area (SolidWorks, Dassault Systèmes SolidWorks Corp., Waltham, USA). This part of the implant, leaning against posterior ledge of the most posterior part (orbital process of palatal bone) became the template for the intra-orbital implant location. This simple procedure makes it possible to avoid surgical navigation in the operating theatre without any loss precision of implant placement.

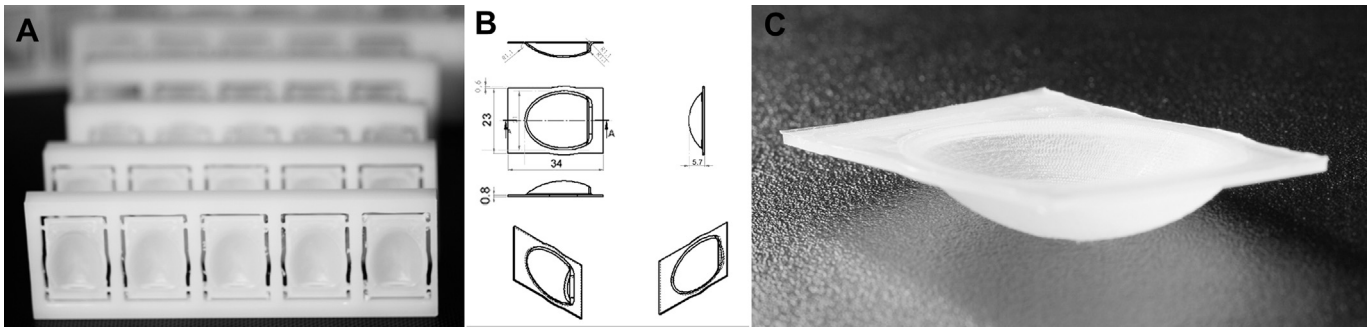

Fig. 1. Shape stability validation. A – series of test implants just after computer assisted milling, B – design of the test implant (dimensions in mm), C – the test implant released from a block of ultrahigh molecular weight polyethylene.

Subsequently, the surface of interest (the injured orbital wall where the implant is to be located) was translated from virtual model data to a CAD program Pathtrace Edgecam (Edgecam, Berkshire, UK) to prepare the model for the milling machine. The virtual implant was inspected by a maxillofacial surgeon. Any sharp edges and angles were removed to decrease intra-operational morbidity. The surface area of the implant had to be carefully evaluated to avoid too short an implant. Then, a corrected virtual implant was approved.

The file was imported to the CAM software (SolidWorks, Dassault Systèmes SolidWorks Corp., Waltham, USA). Appropriate tools and a milling strategy to reproduce the virtual model in the most accurate manner were selected. Finally, a numerical code (NC) was generated for the 5-axis milling machine which manufactured the implants from medical certified UHMW-PE (Ticona Engineering Polymers, USA). Two versions of each implant (e.g. a thicker one and a thinner one) were usually produced from the block. In case of large globe dislocation the implant was designed and milled in suitably bigger dimensions. Later, the milled implants were sent to a surgeon for critical verification. Afterwards, they were corrected, if needed, and sterilized in low temperature conditions.

The placement of the orbital floor implants was made with a standard transconjunctival approach. The surgery was performed under general anaesthesia. Herniated tissues were repositioned and the patient-specific implant was inserted to the orbit. A passive motility test was performed at the end of surgery. A post-surgery functional orthoptic examination and CT scans to confirm the position of the globe were made. The improvement was graded on a 3-grade scale based on BSV loss. The result was considered as "good" when the binocular single vision loss (BSV loss) was less than 0.05. A "moderate" result corresponds to BSV loss of 0.06–0.25. Any results above these values were considered as "poor". Results were evaluated 1-month post-operationally (BSVpost01), 6-month post-operationally (BSVpost06) and 12 months after orbital surgery (BSVpost12).

A statistical evaluation was performed in Statgraphics Centurion XVI which included the summary statistics and an analysis of linear regression. *T*-test was applied for normal distribution and sign test when other distribution was found. These statistics were used for time-dependent changes of vision function. Statistical significance was determined as $p < 0.05$.

3. Results

3.1. Validation of the sterilization process

The results of validation of the sterilization process are presented in Table 1, Fig. 2. Autoclaving deformed the test implants in three of six investigated dimensions, i.e. width (4% shrinkage, $p < 0.05$), length (6% lengthen, $p < 0.05$) and parallel contact with flat surface (corners were raised up). No statistically confirmed deformation of test implants was detected using ethylene oxide sterilization. The gas plasma process involved minimal shrinkage (0.3%) of the implant width ($p < 0.05$). The electron radiation changed only the concavity of the test implants (1.3% deeper concavity after sterilization, $p < 0.05$).

3.2. The implant

After milling, the implants were not polished. Their surface was not porous but became rough. After approval by the maxillofacial surgeon, the implants were packed and sterilized in ethylene oxide at low temperature. The following day the individually designed implants were ready to use.

Depending on the reconstruction strategy, the thickness of implants varied from 0.2 mm to 4.0 mm. The thicker implants were

Table 1
The influence of sterilization procedure to dimensions of ultrahigh molecular weight polyethylene implants.

Feature	CAD	CAM	Autoclave		Ethylene oxide		Gas plasma		Radiation	
	mm	mm	mm	%	mm	%	mm	%	mm	%
Width	23.0 mm	23.09 ± 0.08	22.12 ± 0.09*	−4.06 ± 0.38	23.05 ± 0.04	0.04 ± 0.09	23.06 ± 0.09*	−0.30 ± 0.25	23.15 ± 0.07	0.09 ± 0.18
Length	34.0 mm	34.20 ± 0.10	36.35 ± 0.10*	6.46 ± 0.31	34.27 ± 0.05	0.09 ± 0.23	34.21 ± 0.11	0.15 ± 0.24	34.28 ± 0.10	0.0001 ± 0.15
Deep of concavity	5.7 mm	5.73 ± 0.26	5.34 ± 0.18	−0.78 ± 4.55	5.82 ± 0.20	0.44 ± 2.67	5.84 ± 0.29	0.41 ± 2.16	6.01 ± 0.15*	1.34 ± 0.99
Thickness	0.8 mm	0.86 ± 0.14	0.74 ± 0.11	1.74 ± 14.31	0.95 ± 0.09	1.25 ± 4.60	0.87 ± 0.15	−0.65 ± 3.12	0.90 ± 0.12	−0.68 ± 3.17
Sharpness of corners	Yes	Yes	Yes		yes		yes		Yes	
Parallel contact with flat surface	Yes	Yes	No		yes		yes		Yes	

Abbreviations: mm – data measured in millimetres, % – percentage of measure alteration after sterilization, CAD – designed test implant dimensions, CAM –dimensions of test implants measured prior to sterilization process, * – significant statistical difference between measure before versus after sterilization process.

Table 2
Series of cases treated with patient-specific UHMW-PE implants.

Case	Age	Gender	Reason	ODI	Side	Timing of surgery	Min. implant thickness [mm]	Max. implant thickness [mm]	BSVpre	BSVpost01	BSVpost06	BSVpost12	Surgery duration [h]	Previous orbital surgery	Duration from previous surgery [years]
1	27	M	Assault	2	R	Early	0.5	0.5	0.11	0.08	0	0	0.75	No	
2	28	M	Assault	1	R	Delayed	0.3	0.4	0.04	0.07	0.05	0.01	1.5	Yes	9
3	30	F	Car accident	8	R	Delayed	1.0	4.0	0.45	0.39	0.41	0.19	4	Yes	0.6
4	31	F	Sport accident	5	R	Delayed	1.0	3.5	0.26	0.21	0.14	0.08	2	Yes	0.5
5	32	M	Assault	2	L	Delayed	0.3	0.4	0.18	0.12	0.05	0.02	1	No	
6	20	F	Assault	5	R	Delayed	0.7	1.0	0.17	0.10	0.10	0.03	1	Yes	1
7	30	M	Assault	1	R	Delayed	0.5	0.8	0.1	0.04	0.01	0.01	2	Yes	1.1
8	30	M	Sport accident	1	L	Delayed	0.3	2.0	0.3	0.19	0.10	0.09	1	Yes	0.7
9	24	M	Assault	5	L	Delayed	0.2	2.0	0.28	0.20	0.20	0.11	0.75	No	
10	29	M	Car accident	7	L	Delayed	0.5	1.0	0.27	0.85	0.55	0.31	1.5	Yes	0.9

Legend: ODI-orbital destruction intensity scale; BSVpre-binocular single vision loss before implantation UHMW-PE; BSVpost01-binocular single vision loss one month post-operationally; BSVpost06-binocular single vision loss six months post-operationally; BSVpost12-binocular single vision loss twelve months after surgery.

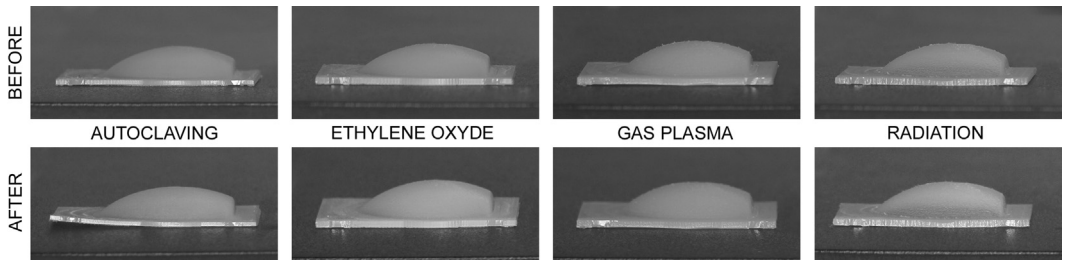

Fig. 2. Shape stability validation. Test implants before and after sterilization process. Visual inspection reveals deformation induced by autoclaving process.

used for eye globe position correction in severely enophthalmic cases. These implants showed satisfactory rigidity and ensured that the globe position was stable. They were necessary in cases which scored high on the orbital destruction intensity scale (Kozakiewicz et al., 2011). On other hand, a thinner implant (0.2 mm) was utilized successively to cover fracture lines and minor orbital wall defect. Therefore, the orbital volume was minimally modified by the volume of the implant.

The minimum thickness of the implant ranged from 0.2 to 1.0 mm and the maximum was 0.4–4.0 mm, depending on the desired orbital wall shape and need to reposition the globe. The average duration of surgery was 1.55 ± 0.98 h, and ranged from 0.75 to 4.0 h. The implant application is presented in Figs. 3–8.

3.3. Preliminary evaluation

There was no infection or extrusion of an implant in the follow-up periods. BSV loss evaluation in the early post-operational period (1-month post-op) classified 1 patient as a good functional result, 7 moderate and 2 as poor. Six months after the surgical treatment, 4 were good, 4 moderate and 2 still poor. The final residual diplopia evaluation revealed 5 cases as good, 4 as moderate and 1 as poor following the treatment.

Generally (Fig. 9), early functional results did not differ from the pre-operative diplopia (BSVpre vs BSVpost01: test statistic = 1.58, $p = 0.11$; BSVpre vs BSVpost06: test statistic = 1.34, $p = 0.21$; BSVpost01 vs BSVpost06: test statistic = 1.77, $p = 0.053$), only late results revealed improvement of vision (BSVpre vs BSVpost12: test statistic = 4.72, $p < 0.01$; BSVpost06 vs BSVpost12: test statistic = 2.77, $p < 0.05$).

Simple regression analysis revealed a moderately strong relationship between BSVpre and BSVpost01 (correlation coefficient cc = 0.79, $R^2 = 62\%$, $p < 0.01$), BSVpre and BSVpost06 cc = 0.76, $R^2 = 58\%$, $p < 0.05$), BSVpre and BSVpost12 (cc = 0.80, $R^2 = 65\%$, $p < 0.01$) – Fig. 10. The progress of rehabilitation was presented in post-operational results: BSVpost01 and BSVpost06 (cc = 0.97, $R^2 = 95\%$, $p < 0.0001$), BSVpost06 and BSVpost12 (cc = 0.98, $R^2 = 97\%$, $p < 0.0001$), and BSVpost01 and BSVpost12 (cc = 0.99, $R^2 = 98\%$, $p < 0.0001$). The result of treatment was independent from the patients' age. Types of injury effects, classified by an orbital destruction intensity scale, were moderately related to the initial diplopia (cc = 0.78, $R^2 = 62\%$, $p < 0.01$), to the results of the treatment (ODI and BSVpost01: cc = 0.80, $R^2 = 64\%$, $p < 0.01$; ODI and BSVpost06: cc = 0.90, $R^2 = 80\%$, $p < 0.001$; ODI and BSVpost12: cc = 0.81, $R^2 = 66\%$, $p < 0.005$) and to the thickness of implants produced (ODI and maximal thickness cc = 0.64, $R^2 = 42\%$, $p < 0.05$; ODI and minimal thickness cc = 0.63, $R^2 = 39\%$, $p = 0.053$). Larger injuries led to longer surgical procedures (ODI and Surgery duration: cc = 0.68, $R^2 = 47$, $p < 0.05$).

The minimum thickness of the used implant was independent from the initial diplopia (cc = 0.57, $R^2 = 32\%$, $p < 0.008$), contrary to the maximum thickness which was moderately related to the initial diplopia (cc = 0.78, $R^2 = 61\%$, $p < 0.01$). The minimum implant thickness did not influence the post-operational diplopia level (1 month after surgery: cc = 0.30, $R^2 = 9\%$, $p = 0.39$, 6 months: cc = 0.36, $R^2 = 13\%$, $p = 0.31$, 12 months: cc = 0.31, $R^2 = 10\%$, $p = 0.38$), similarly the maximum thickness (1 month: cc = −0.56, $R^2 = 31\%$, $p = 0.09$, 6 months: cc = −0.57, $R^2 = 35\%$, $p = 0.07$). The only exception was the patients' condition 12 months after surgery: cc = −0.66, $R^2 = 44\%$, $p < 0.05$. Duration of the surgical procedure was related to the initial level of diplopia (cc = 0.79, $R^2 = 63\%$, $p < 0.01$), but longer surgery did not reduce functional results in any investigated period (BSVpost01 and Surgery duration: cc = 0.33, $R^2 = 11\%$, $p = 0.35$; BSVpost06 and Surgery duration: cc = 0.48, $R^2 = 23\%$, $p = 0.16$; BSVpost12 and Surgery duration: cc = 0.40, $R^2 = 16\%$, $p = 0.25$).

4. Discussion

The main medical use of ultrahigh molecular weight polyethylene (UHMW-PE) is in orthopaedics. UHMW-PE has rapidly gained wide acceptance in total joint arthroplasty due to

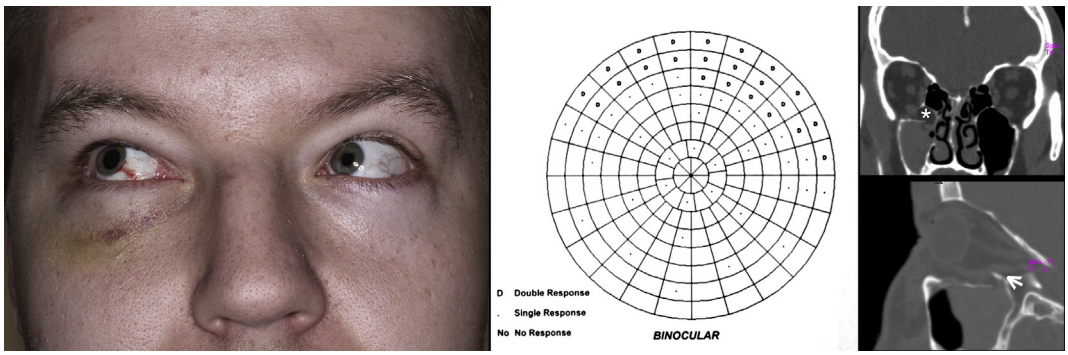

Fig. 3. Patent 3 days after injury (case #1). Blowout fracture of the right orbit. Upgaze limited (in the left picture). In the centre: Binocular Single Vision test pre-operationally. Double vision upgaze (D). In the right: Multiplanar reconstruction of computerized tomography imaging (MPR): the upper radiograph presents coronal plane with lower orbital wall bone defect involving lower rectus muscle in the right orbit (asterix); sagittal plane – the muscle is pricked by the bone edge in the distal part of the orbit (arrow).

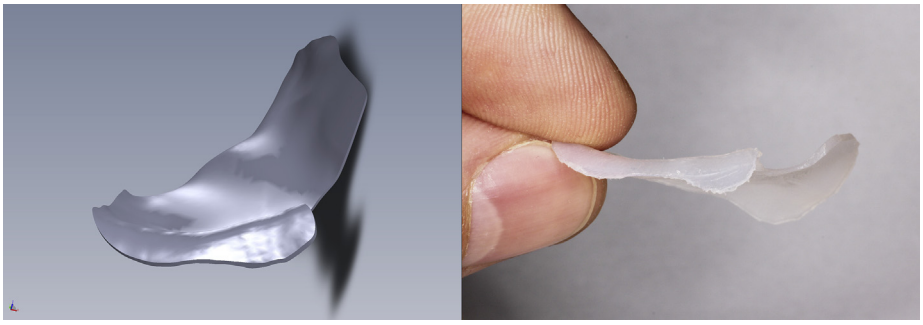

Fig. 4. In the left: Virtual project of the implant made based on mirrored intact orbit. The anterior cuff is the localization marker of the implant. It covers the lower orbital rim to fix the implant in strictly planned spatial orientation. In the right: Solid raw implant (just after manufacture in CNC milling machine) produced of ultrahigh molecular weight polyethylene.

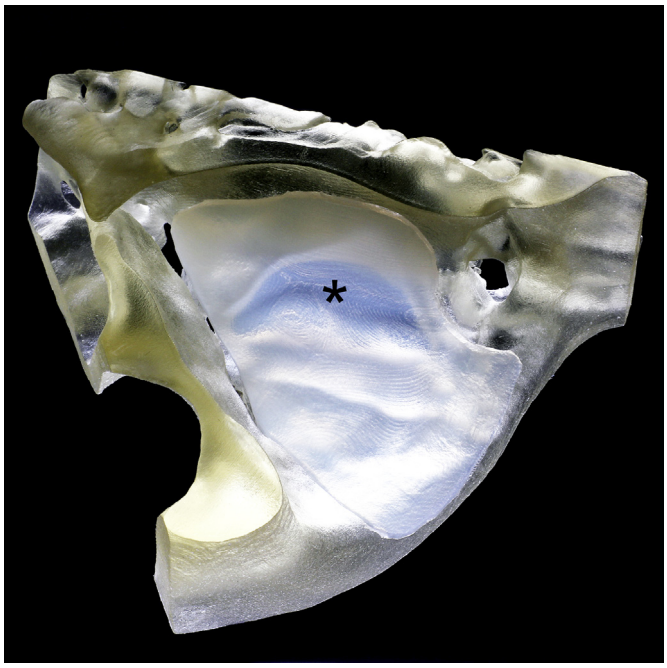

Fig. 5. Final custom implant located in the rapid prototyped individual model. Surface-to-surface alignment is completed. Less than half-a-millimetre implant is partially translucent – the bone defect is located just below the implant (asterisk).

remarkably low wear and the associated lack of periprosthetic osteolysis. Negligible wear of UHMW-PE in both hip and knee for durations simulating 20 years of in vivo service has been shown (Jasty et al., 2005). The stiffness of the polymer seems to be a suitable physical feature for orbital reconstruction. Ultrahigh molecular weight polyethylene (UHMW-PE) provides a combination of excellent properties: outstanding abrasion resistance, superior impact resistance, non-sticking and self-lubricating features and excellent mechanical characteristics. It is a polymer of extremely high viscosity that is produced in the form of a powder and has an average particle size diameter ranging from 100 to 200 μm. As a result of its viscosity, it generally cannot be processed by the common methods used for ordinary thermoplastics. Thus, compression moulding and ram extrusion processes are used to generate the high pressures needed to fuse UHMW-PE particles together and then, typically, to form the material into stock shapes or profiles followed by subsequent machining, as necessary (Ticona Engineering Polymers, 2011).

Alloplastic materials have been shown to reduce the number of bacteria required to produce infection by a factor of 10^4–10^6 (Sclafani et al., 1997). The nonporous surface of the custom UHMW-PE implant makes it more resistant to intra-operational infection. The material has some of the features of polytetrafluoroethylene (PTFE) (Sclafani et al., 1997). On the other hand, the very slightly rough surface makes the implant more resistant to late infections because superficial fibrovascularization encourages increased immune response mediators at this expanded surface of alloplast (Zimmerli et al., 1982).

The previously described technical concept of UHMW-PE patient-specific orbital wall implants made it possible to tailor implants to specific intra-operational needs (Kozakiewicz et al., 2013). The material is radiolucent on CT scans and MRI images, causing no interference with post-operative imaging, although in a combination with a radio-opaque component, embedded or covering, it may be useful in radiographic follow-up examination (Liu et al., 2004). Looking for thin polyethylene implants was the next desirable

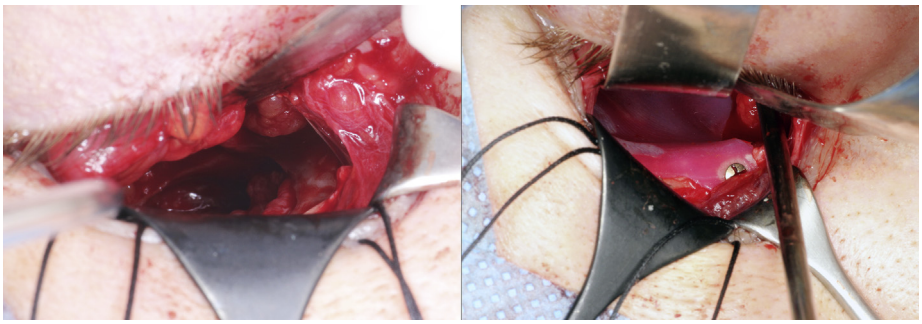

Fig. 6. In the left: Intra-operational view to the lower orbital wall through tranconjuctival approach. Bone defect length 2 cm and width 1.5 cm. Herniated tissues were translocated into the orbit. In the right: Custom ultrahigh molecular weight polyethylene implant located in the orbit according to the guidance of the anterior cuff. Titanium screws stabilized the implant in its cuff on the lower orbital rim.

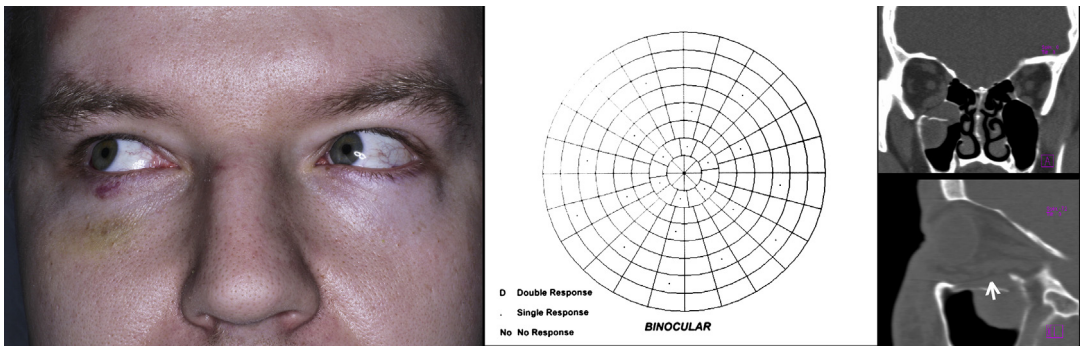

Fig. 7. Patient after surgery. Full upgaze motility (in the left picture). In the centre: Binocular Single Vision test post-operationally. No double vision. In the right: Post-operational computerized tomography (MPR in coronal and sagittal planes). Ultrahigh molecular weight polyethylene implant is not radio-opaque. Its location is presented as low density line in lower orbital wall in the right site. Lower orbital muscle runs along proper silhouette of orbital floor (arrow).

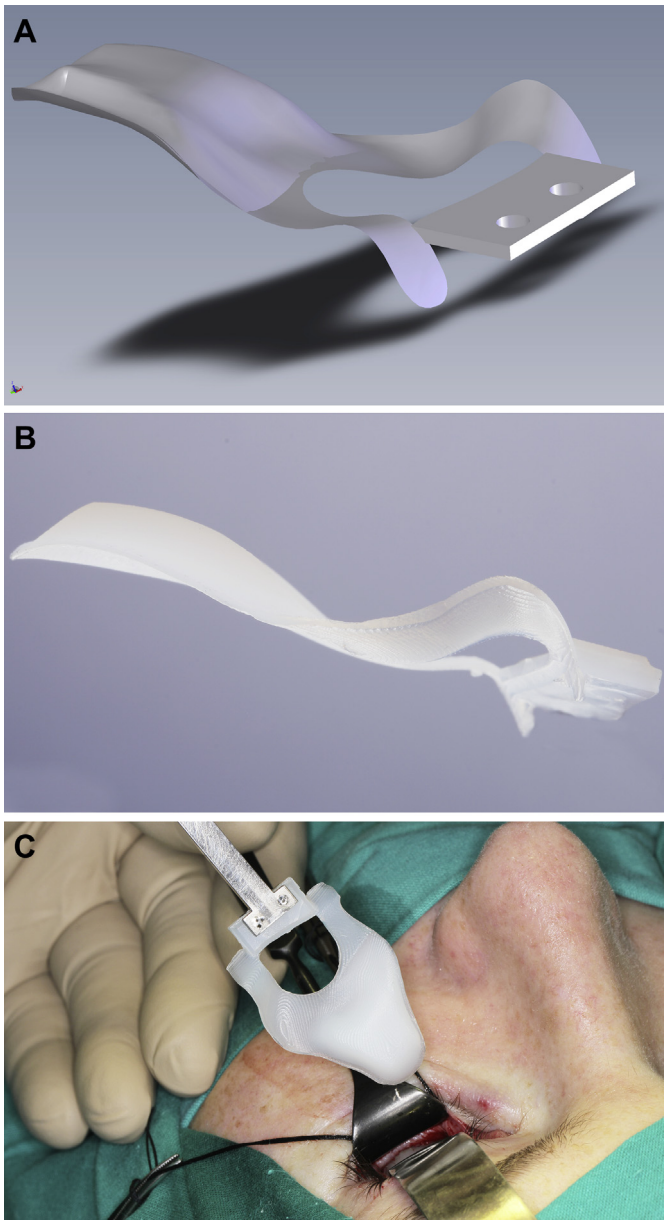

Fig. 8. Patient specific, thickness modulated, UHMW-PE implant (case #10). A – computer assisted design; implant with significant higher thickness in posterior part contrary to thin anterior part; in the central part concavity for eye globe; note: light implant part connections. B – manufactured solid implant according to CAD guide. C – Implant insertion to the orbit.

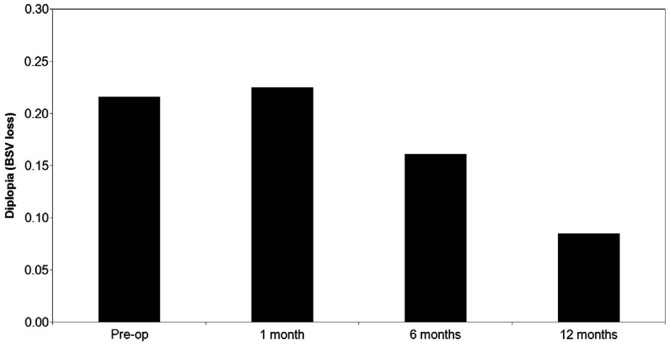

Fig. 9. Average binocular single vision loss before (Pre-op) and after treatment with UHMW-PE patient-specific implants in series of delayed treated orbital fractures. Diplopia (BSV loss) range is from 0 (normal vision) to 1 (whole vision field affected by diplopia).

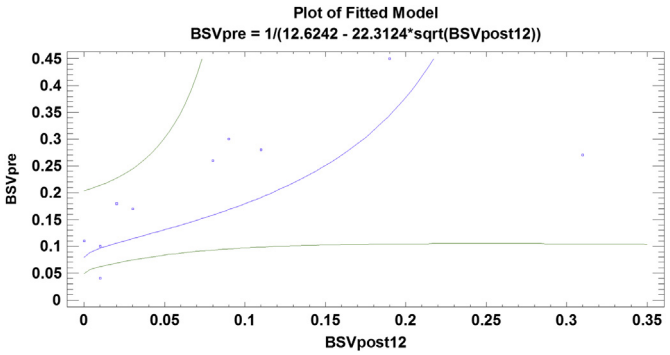

Fig. 10. Results of treatment with UHMW-PE implant (BSVpost12) depends on the initial level of posttraumatic diplopia (BSVpre). Result of treatment definitely depended on the level of posttraumatic vision dysfunction (significant relation $p < 0.01$, correlation coefficient cc = 0.8). Green lines – confidence limits (95% patients' results are included in the surface area limited by the green lines).

feature (Ozturk et al., 2005). Now, we can produce a patient-specific implant, thin or with individually variable thickness, made from a durable biocompatible polymer.

The method of sterilization can alter the shape of the implant. Autoclaving is not a good technique for UHMW-PE implant sterilization, but other methods of sterilization can be considered. It was shown that the ethylene oxide process affected the dimensions of implant to the least extent. It should be emphasized that even in 134 °C, the test implants did not melt.

In delayed and multisurgical cases, functional results of orbital surgery are worse than in simpler cases (Kozakiewicz et al., 2011),

but in long-term follow-up, the resolution of diplopia is noticeable. The outcomes of treatment depend on the initial level of diplopia (analysis of regression has shown a positive correlation), and correction of severe initial diplopia required thicker implants. This means that larger orbital wall defects need larger reduction (moderately strong relation, $p < 0.01$). This also leads to longer surgical procedures ($p < 0.01$), but longer surgery has no negative influence upon results of any investigated follow-up examinations. What is obvious, orbital destruction intensity is related to the initial diplopia caused by injury, but it also influences the entire results of the treatment up to 12 months post-op.

The relation of the maximum implant thickness to 12-month diplopia is interesting. Using thicker implants results in lower residual diplopia ($p < 0.05$). This is important because the higher orbital destruction intensity correlates to thicker UHMW-PE implant ($p < 0.05$) applied in this series. Thus, a surgeon should not be afraid of a significant eye globe repositioning caused by patient specific, thickness modulated, implants. It helps in efficient correction of enophthalmos.

Enophthalmos in posttraumatic cases is determined by the enlargement of the orbital cavity, the herniation of orbital fat into sinuses, fat atrophy, loss of ligament support and scar contracture. Restoration can be achieved in treatment with bone grafts harvested from calvaria or iliac crest or with biomaterials (Clauser et al., 2008). Adequate hard tissue reconstruction is fundamental for correction of the enophthalmos. Long-term outcomes of standard polyethylene implants used for reconstruction of orbital floor defects showed 7–11% persistence of enophthalmos, and, in 6–17%, diplopia (Hoşal and Beatty, 2002, Ozturk et al., 2005). These final results suggest we need to look for new treatment methods. Patient-specific alloplastic implants are promising for our team (poor result concerning diplopia represents 10%). This is the first step to check if this material and technique will be accepted in the future.

The proposed implantation material and method has both advantages and disadvantages. Advantages include: restoration of the original shape of the orbital wall, excellent structural support combined with a thin implant, the ability to treat large orbital floor defects, possible modification of local implant thickness on the level of CAD design, easy and precise in use, using a CAD model of the implant as an intrasurgical navigation tool (with compatible neuronavigation devices), mild edges and transitions from thin to thick parts of the implant, freely located perforations protect the implant against movements in site (for example: perimeter line perforation or one margin perforation), easy intra-operational correction by scissor/blade cut, minor morbidity, and no interference with MRI or CT imaging. The last feature makes it possible to evaluate extraocular muscles, but simultaneously it is a disadvantage because one is not able to inspect implant position inside the orbit. Other disadvantages are: no possibility to enlarge or alter concavity of the implant during surgery (manufacture of a larger size implant than the planned dimensions of the implant is mandatory), a fixing screw is needed to stabilize during the first phase of healing (in larger defects) and time expenditure for design and production (pre-operationally).

5. Conclusion

Patients-specific ultrahigh molecular weight polyethylene implants enable precise reconstruction of orbital walls. One should not be afraid of a significant eye globe reposition caused by these thickness modulated implants, as such repositioning is essential for an efficient correction of enophthalmos.

Financial support

Medical University of Lodz grant 503/5-061-02/503-01, Ledo Company [www.ledo.pl].

References

Betz MW, Caccamese JF, Coletti DP, Sauk JJ, Fisher JP: Challenges associated with regeneration of orbital floor bone. Tissue Eng Part B Rev 16: 541–550, 2010
Brady SM, McMann MA, Mazzoli RA, Bushley DM, Ainbinder DJ, Carroll RB: The diagnosis and management of orbital blowout fractures: update 2001. Am J Emerg Med 19: 147–154, 2001
Clauser L, Galiè M, Pagliaro F, Tieghi R: Posttraumatic enophthalmos: etiology, principles of reconstruction, and correction. J Craniofac Surg 192: 351–359, 2008
Frodel JL, Lee S: The use of high-density polyethylene implants in facial deformities. Arch Otolaryngol Head Neck Surg 124: 1219–1223, 1998
He D, Li Z, Shi W, Sun Y, Zhu H, Lin M, et al: Orbitozygomatic fractures with enophthalmos: analysis of 64 cases treated late. J Oral Maxillofac Surg 70: 562–576, 2012
Hoşal BM, Beatty RL: Diplopia and enophtalmos after surgical repair of blowout fracture. Orbit 21: 27–33, 2002
Hwang K, You SH, Sohn IA: Analysis of orbital bone fractures: a 12-year study of 391 patients. J Craniofac Surg 20: 1218–1223, 2009
Jasty M, Rubash HE, Muratoglu O: Highly cross-linked polyethylene: the debate is over-in the affirmative. J Arthroplasty 20: 55–58, 2005
Kashkouli MB, Pakdel F, Sasani L, Hodjat P, Kaghazkanani R, Heirati A: High-density porous polyethylene wedge implant in correction of enophthalmos and hypoglobus in seeing eyes. Orbit 30: 123–130, 2011
Kirby EJ, Turner JB, Davenport DL, Vasconez HC: Orbital floor fractures: outcomes of reconstruction. Ann Plast Surg 66: 508–512, 2011
Kozakiewicz M, Elgalal M, Walkowiak B, Stefanczyk L: Technical concept of patient-specific, ultrahigh molecular weight polyethylene, orbital wall implant. J Craniomaxillofac Surg 41: 282–290, 2013
Kozakiewicz M, Elgalal M, Loba P, Komunski P, Arkuszewski P, Broniarczyk-Loba A, et al: Clinical application of 3D pre-bent titanium implants for orbital floor fractures. J Craniomaxillofac Surg 37: 229–234, 2009
Kozakiewicz M, Elgalal M, Loba P, Broniarczyk-Loba A, Stefanczyk L: Treatment with individual orbital wall implants in humans – 1-year ophthalmologic evaluation. J Craniomaxillofac Surg 39: 30–36, 2011
Lee S, Maronian N, Most SP, Whipple ME, McCulloch TM, Stanley RB, et al: Porous high-density polyethylene for orbital reconstruction. Arch Otolaryngol Head Neck Surg 131: 446–450, 2005
Liu JK, Gottfried ON, Cole CD, Dougherty WR, Couldwell WT: Porous polyethylene implant for cranioplasty and skullbase reconstruction. Neurosurg Focus16 3, 2004
Loba P, Kozakiewicz M, Elgalal M, Stefanczyk L, Broniarczyk-Loba A, Omulecki W: The use of modern imaging techniques in the diagnosis and treatment planning of patients with orbital floor fractures. Med Sci Monit 17: CS94–CS98, 2011
Ozturk S, Sengezer M, Isik S, Turegun M, Deveci M, Cil Y: Long-term outcomes of ultra-thin porous polyethylene implants used for reconstruction of orbital floor defects. J Craniofac Surg 16: 973–977, 2005
Rhim CH, Scholz T, Salibian A, Evans GR: Orbital floor fractures: a retrospective review of 45 cases at a tertiary health care center. Craniomaxillofac Trauma Reconstr 31: 41–47, 2010
Schön M, Metzger C, Zizelmann C, Weyer N, Schmelzeisen R: Individually preformed titanium mesh implants for a true-to-original repair of orbital fractures. Int J Oral Maxillofac Surg 35: 990–995, 2006
Sclafani AP, Thomas JR, Cox AJ, Cooper MH: Clinical and histologic response of subcutaneous expanded polytetrafluoroethylene gore-tex and porous high-density polyethylene medpor implants to acute and early infection. Arch Otolaryngol Head Neck Surg 123: 328–336, 1997
Tabrizi R, Ozkan TB, Mohammadinejad C, Minaee N: Orbital floor reconstruction. J Craniofac Surg 21: 1142–1146, 2010
Ticona Engineering Polymers: 8040 Dixie Highway, Florence, KY 41042, USA. http://www.celanese.com/ticona/products/GUR-UHMW-PE.aspx, 2011 [accessed 21.10.12].
Wajih WA, Shaharuddin B, Razak NH: Hospital Universiti Sains Malaysia experience in orbital floor reconstruction: autogenous graft versus Medpor. J Oral Maxillofac Surg 69: 1740–1744, 2011
Wu W, Yan W, Cannon PS, Jiang AC: Endoscopic transethmoidal and transconjunctival inferior fornix approaches for repairing the combined medial wall and orbital floor blowout fractures. J Craniofac Surg 22: 537–542, 2011
Xu JJ, Teng L, Jin XL, Ji Y, Lu JJ, Zhang B: Porous polyethylene implants in orbital blow-out fractures and enophthalmos reconstruction. J Craniofac Surg 203: 918–920, 2009
Zimmerli W, Waldvogel FA, Vaudaux P, Nydegger UE: Pathogenesis of foreign body infection: description and characteristics of an animal model. J Infect Dis 146: 487–497, 1982